

Proceeding Paper

Development of a Corrosion Protection Silica-Based Hybrid Sol-Gel Coatings on Aluminum Alloys 2024-t3 by Encapsulating Benzimidazole and Octadec-9-Enoic Acid [†]

Magdi Hassn Mussa ^{1,2,3,*}, Sarra A. Takita ⁴, Nicholas Farmilo ⁴ and Oliver Lewis ⁴

¹ Mechanical and Energy Department, The Libyan Academy for Graduate study, Tripoli P.O. Box 79031, Libya

² Mechanical Engineering Department, Sok Alkhamis Imsehel High Tec. Institute, Tripoli P.O. Box 79031, Libya

³ The Institute of Marine Engineering, Science and Technology, London SW1H 9JJ, UK

⁴ Materials and Engineering Research Institute MERI, Sheffield Hallam University, Howard Street, Sheffield S1 1WB, UK; Sarah.a.takita@gmail.com (S.T.); O.Lewis@shu.ac.uk (O.L.); nfarmilo@gmail.com (N.F.)

* Correspondence: magdimosa1976@gmail.com; Tel.: +447404496955.

[†] Presented at the 26th International Electronic Conference on Synthetic Organic Chemistry; Available online: <https://ecsoc-26.sciforum.net>.

Abstract: Corrosion affects any metallic materials, such as pipelines, ships, and offshore platforms, as it is estimated that year's corrosion losses are one-fifth of the global resources. The most efficient way of reducing the impact of this environment is using coatings- provision of barrier between the material and the aggressive environment. Hybrid Silica-based Sol-gel-derived coating presents one of the most viable pre-treatments alternatives to chromate. A significant advantage of the sol-gel process is the possibility of forming a hybrid inorganic-organic structure network at low temperatures. In addition, sol-gel coatings have good adhesion to metallic substrates and organic materials. Therefore, as a continuance of previous research on sol-gel coating systems. The work reports the performance of hybrid sol-gel formula formed from TEOS and MTMS enhanced by polysiloxanes with and without the presence of environmental benign corrosion inhibitor individually formed from benzimidazole (BZI) and Octadec-9-enoic acid (OA) as a duplex layer's coating system. The sol-gel only and the duplex coating systems were at the same thickness, which can be applied to lightweight alloys such as aluminum alloy 2024-t3 to form a fundamentally corrosion-inhibited and crack-free coating. The corrosion protection mechanism's evaluation for these coatings is based on electrochemical tastings using potential-dynamic polarization scanning (PDPS) and electrochemical impedance spectroscopy (EIS). The protective properties of the coating system were studied when immersed in 3.5% NaCl to imitate the aggressive environment. The chemical confirmation was checked by infrared spectroscopy (FTIR), supported by analyzing surface morphology after 360 h. of immersion testing using scanning electron microscopy (SEM) and water contact angle for coated samples (WCA). The corrosion resistance performance of this coating system is a result of the combination of good adhesion and pore blocking of the silica-based hybrid coating and the presence of both encapsulated OA as a carrier and BZI as a film-forming volatile corrosion inhibitor resulting in durable film-forming, reducing the reaction at cathodic sites. Also, it exhibited excellent anti-corrosion properties, providing an adherent protective film on the aluminum alloy 2024-T3 samples compared to previous sol-gel and bare metals, which might last more than 60 days without any sign of failure, with an eco-friendly and cost-effective.

Keywords: hybrid silica-based sol-gel coating; electrochemical testing; corrosion protection; aluminum alloys; benzimidazole; Octadec-9-enoic

Citation: Mussa, M.H.; Takita, S.A.; Farmilo, N.; Lewis, O. Development of a Corrosion Protection Silica-Based Hybrid Sol-Gel Coatings on Aluminum Alloys 2024-t3 by Encapsulating Benzimidazole and Octadec-9-enoic Acid. *2022*, *4*, x. <https://doi.org/10.3390/xxxxx>

Academic Editor(s): Julio A. Seijas

Published: 15 November 2022

Publisher's Note: MDPI stays neutral with regard to jurisdictional claims in published maps and institutional affiliations.



Copyright: © 2022 by the authors. Submitted for possible open access publication under the terms and conditions of the Creative Commons Attribution (CC BY) license (<https://creativecommons.org/licenses/by/4.0/>).

1. Introduction

Aluminum alloys, especially AA2024-T3, are widely used in aerospace and marine offshore structural industries because of their high specific strength ratio and their moderate cost. Due to this, the element of copper in these alloys is used to improve their mechanical stiffness. However, this, in turn, can result in microscopic galvanic couples, which increase the potential for corrosion on these alloys. Therefore, to avoid localized corrosion that could damage the mechanical properties of metallic structures, the general technique is to prevent the direct interaction of the electrochemically active matrix with the environment by applying a protective coating system to prolong the service life of parts before applying a painting application. In addition, the alloy is frequently clad or anodized to provide good bonding between the paint and the substrate [1,2]. There are possibly numerous applications in industries involving sol-gel-derived technologies. The sol-gel processes can produce various materials, including coatings, films, fibers, monoliths, and nanosized powders. Coatings or thin films produced by the sol-gel technology are typical of early commercial involvement. Other examples of coating applications of the sol-gel films include self-cleaning coatings, hydrophobic coatings, and anti-corrosion and wear-resistance coatings [3–6]. Hybrid sol-gel protective coatings technology has shown an exceptional ability to mitigate corrosion on the metal surface combined with high chemical stability. Nevertheless, using the sol-gel method only as a protective coating has some limitations in terms of barrier anti-corrosive properties due to pores in the matrix, which could lead to cracking of the coating and make protection fail in the end. The encapsulation technology of corrosion inhibitors will enhance the system's corrosion protection. The systematic development of corrosion inhibitor compounds has produced many effective inhibitors [7,8]. For example, compounds with heterocyclic organic functional groups consisting of oxygen or nitrogen, with phosphorus or sulfur attached as heteroatoms, are very desirable spatially if combined with a fatty acid carrier [9,10]. For instance, the last paper studied benzimidazole (BZI) as a low-pH film-forming effective corrosion inhibitor to protect aluminum alloys 2024-t3. Moreover, it revealed good protection and excellent stability with sol-gel coating [11]. octadec-9-enoic acid (OA) is considered one of the recommended fatty acids mentioned previously in the US forces report from 1991 for use as a corrosion inhibitor or inhibitor carrier [12]. Although the previous studies studied functional corrosion inhibition of benzimidazole and/or fatty acid on steel alloys only, but the term of use of OA and BZI as encapsulated as well as duplex layers sol-gel will be investigated in this work

2. Materials and Methods

2.1. Synthesizing of Sol-Gel

The hybrid silica-sol-gel was basically prepared from trimethoxymethyl silane (MTMS), and tetraethylorthosilicate silane (TEOS) bought from Merck Sigma-Aldrich, enhanced by polysiloxane as mentioned in the previous study [2,13]. This formulation was used as the original coating and labeled SHX-80. The duplex system, which is labeled as BZI-OA-SHX-80, was made from two layers, the first from Octadec-9-enoic acid made by encapsulating 0.15 vol.% of solution 1:1 of ethanol and OA mixed into the original SHX-80 liquid formula. The other layer was made from benzimidazole, and prepared by encapsulating 3.5 vol/w % of a 1:1 solution of ethanol and BZI (Sigma-Aldrich) in the same base formula, added dropwise while stirring. Both formulations were left for 24 h to complete their hydrolyzing and condensing. Figure 1 shows the process of sol-gel coating.

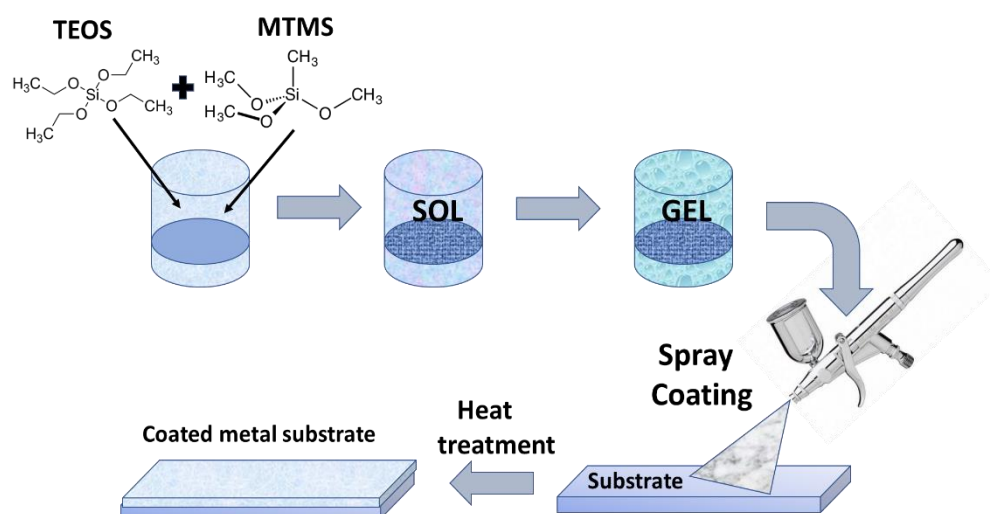


Figure 1. Schematic representation of the sol-gel coatings process [11].

2.2. Substrate Preparation

The Q-panels aluminum alloy AA2024-T3 used as test substrates with sizes of (102 mm × 25 mm × 1.6 mm) were purchased from Q-Lab [14,15]. First, the received panel's substrates were cleaned with the industrial aluminum base surfactant cleaner, according to the mentioned protocol in [3,15]. To keep coatings thickness in standard ranges, with about four passes, the distance from the spray handgun to the substrate surface was around 15 cm until built up; the coating thickness was about 20 μm ±2. Then, coated samples of sol-gel only and OA sol-gel were dried in air for ten minutes before being annealed at 80° C. On the other hand, The duplex system was made by keeping the thickness of the first layer of OA sol-gel at about 10 μm ±2 by applying two passes and the top layer of BZI sol-gel at the same with an overall thickness of 20 μm ±2 as it showed in Figure 2. Table 1 shows the experimentation sample identification codes.



Figure 2. schematic of the double layer sol-gel coating system of BZI and OA, and SEM cross-section image of BZI-OA-SHX sol-gel coating system.

Table 1. Sample identification table.

No.	Identifier	Formula Base Composite	(BZI)	(OA)	Curing Temperature
1-	SHX-80 (monolayer)	TEOS + MTMS	-	-	80 °C
2-	OA-SHX-80 (monolayer)	TEOS + MTMS	-	1.5%	80 °C
3-	BZI-SHX-80 (mono-layer)	TEOS + MTMS	3.5%	-	80 °C
4-	BZI-OA-SHX-80 (duplex-layer)	TEOS + MTMS	3.5%	1.5%	80 °C
5-	Bare AA2024-T3	-	-	-	-

3. Results and Discussion

3.1. ATR-FTIR Results

Confirmation of Benzimidazole in the Sol-Gel Top Layer

The organic component of BZI was incorporated into the SHX sol-gel base formula by comparing the infrared spectrum (ATR-FTIR) obtained from the BZI-SHX-80 coating to that of the unmodified SHX-80, as clearly mentioned in the previous work [13]. Correspondingly, the aromatic amine stretching C–N fingerprint can be detected at 1300 cm^{-1} and 1364 cm^{-1} , respectively, which can confirm the benzimidazole's presence in the new sol-gel formula. Furthermore, the C–H out-of-plane bending is characterized by peaks at 745 cm^{-1} and 768 cm^{-1} [13].

3.2. Water Contact Angle (WCA)

As shown in Figure 3, The results of the measured WCA show that the original monolayer SHX-80 sol-gel coatings were about $67^\circ \pm 2$. The measured WCA on OA-SHX-80 Sol-gel coatings was about 102° , which shows the higher water contact angle recorded for the OA-SHX-80 demonstrates that the OA-SHX-80 Sol-gel coating is less wettable than the base SHX-80 sol-gel coating [16]. While the duplex system as the top layer is BZI-SHX sol-gel, the results of WCA were presented in that layer at about $88^\circ \pm 2$, which is still considered less wettable than the base sol-gel coating.

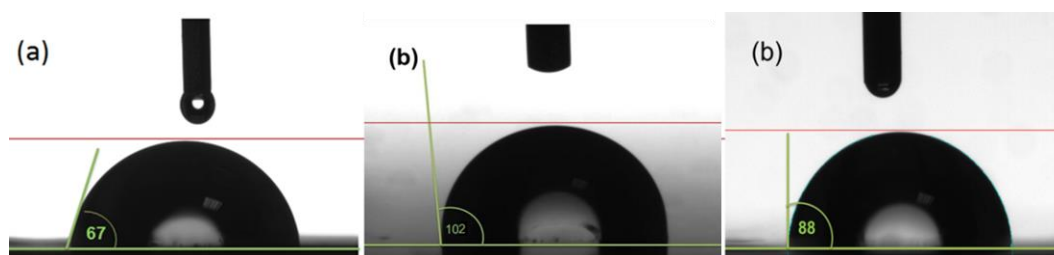


Figure 3. typical WCA Optical images of water drops on surface (a) SHX-80 and (b) modified OA-SHX-80 (c) BZI-OA-SHX-80 coatings system.

3.3. Potential Dynamic Polarization Scanning (PDPS)

The PDPS was used as a primary corrosion protection test to show the performance properties of the coated samples compared to the non-coated bare AA2024 substrates in 3.5% *w/v* NaCl electrolyte solution. The corrosion current density (I_{corr}) and The corrosion potential (E_{corr}) were obtained from the curves shown in Figure 4. Generally, the current density on the cathodic branch of the Tafel curve for all sol-gel coated samples is reduced by more than four magnitudes when compared to the bare AA2024-T3. Nevertheless, from the anodic polarisation curve, the behavior of the four types of coatings was distinct from each other. This returns to the type of inhibitors. First, starting the double-layer benzimidazole/Octadec-9-enoic acid sol-gel system coded as BZI-OA-SHX-80 displayed a more significant reduction, being eight orders of magnitude lower than the current density. Then the benzimidazole sol-gel BZI-SHX-80 coated sample comes second, as it is reduced by seven orders of magnitude to bare AA2024-T3, which may be attributed to benzimidazole's surface-active and high electronegativity [17].

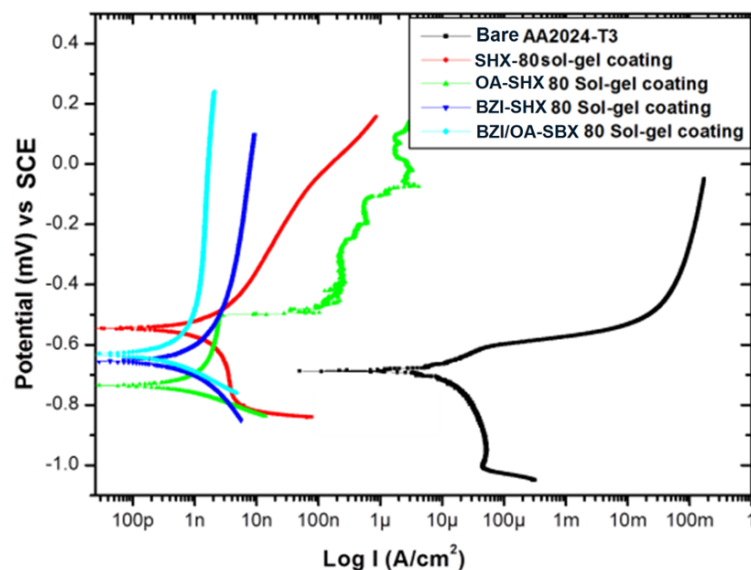


Figure 4. Polarization curves for the sol-gel coated systems in 3.5% NaCl.

On the other hand, the sol-gel with OA inhibitor sample OA-SHX-80 sol-gel showed less protection on the anodic branch, revealing the failure in protection in the potential of -502 mV due to the initiation of pitting and coating failure. This reduction is about four orders of magnitude less than the bare AA 2024-T3. In addition, the SHX-80 sol-gel only showed a fall in the anodic branch by about four and a half orders of magnitude, which is less than the bare AA 2024-T3.

The information obtained from the figure of Corrosion current densities of bare and sol-gel coated samples were reduced to $2.92 \times 10^{-10} A/cm^2$ for (BZI-OA-SHX-80), $5.98 \times 10^{-10} A/cm^2$ for (BZI-SHX-80), $9.8 \times 10^{-10} A/cm^2$ for (OA-SHX-80) and $1.1 \times 10^{-9} A/cm^2$ for (SHX-80) respectively, and as compared to $7.1 \times 10^{-6} A/cm^2$ of the bare AA2024-T3 alloy. This corrosion potential shifted to more positive values for coatings containing BZI and more negative values for those containing Octadec-9-enoic acid.

As a result, the shift in E_{corr} indicates that the anodic is inhibited to a greater degree than the cathode in BZI-OA-SHX 80 and BZI-SHX 80 sol-gel mixture. This is attributed to the benzimidazole nitrogen active atoms bridging to the substrate surface [17,18]. Also, it can be attributed that Octadec-9-enoic acid can clog pores by increasing the hydrophobicity in the filled pores, which contributes to a reduction in the electrolyte diffusion to the surface of the substrate [19,20].

3.4. Impedance Magnitude Bode Plots for Duplex BZI/OA Layers Sol-Gel Coatings

Tests were performed over 1440 h. Figure 5a,b show impedance magnitude and phase angle plots for BZI-OA-SHX-80 duplex coating systems. The general behavior of the coating is as an active corrosion-protective double-layer coating system with good capacitative behavior.

After 24 h. immersion, the impedance at the high frequency of 10^5 Hz starts from about 0.8×10^3 ohms. cm^{-2} reflecting the solution/coating interface resistance (R_s). Then the impedance rises, reflecting that capacitative behavior attributed to coating protection and diffusion resistance. This reading reaches a higher magnitude at the low frequencies between 10 to 0.01 Hz with a value of about 5.0×10^6 ohms. cm^{-2} .

After 72 h of immersion, there is a slight decrease in the impedance attributed to the slow diffusion in the coating to the metal surface, but it still maintains the same protection range.

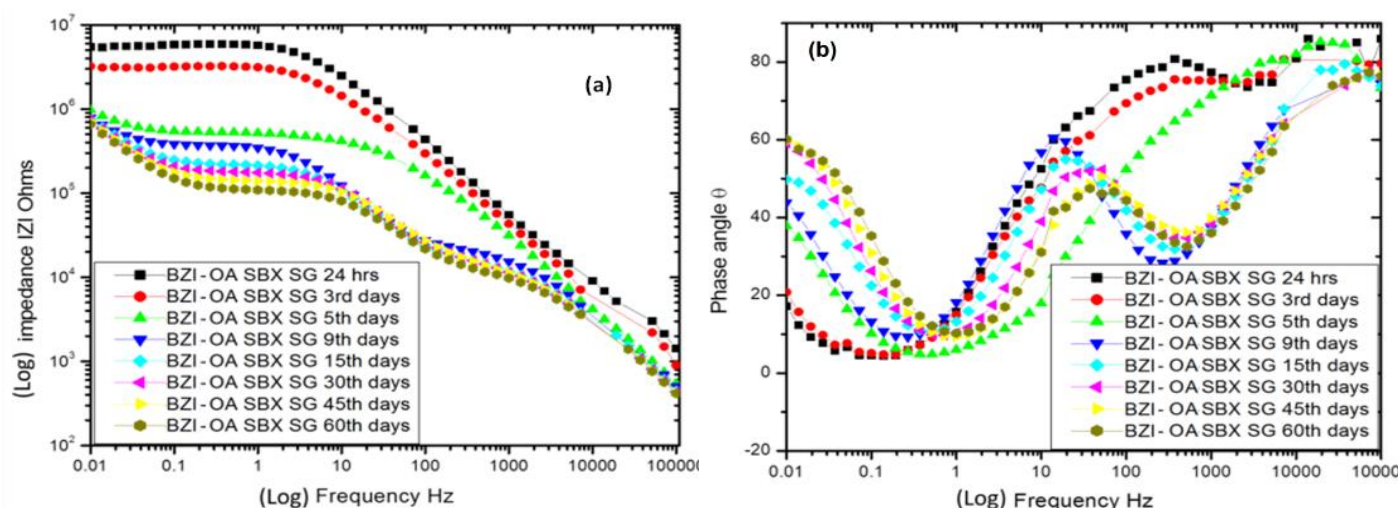


Figure 5. (a) impedance Poda diagram and (b) phase diagram of the duplex system of BZI-OA-SHX-80.

After 120 h of immersion, it decreases significantly to about 1.2×10^6 ohms \cdot cm² at low frequencies. The coating system continues to provide reasonable protection to reach after 216 h, about 9.0×10^5 ohms \cdot cm². It kept this behavior with a minimal drop in impedance until 60 days with an overall magnitude of 7.1×10^5 ohms \cdot cm².

Correspondingly, the phase angle θ Figure 6b showed two time-constants on the first immersion day, reflecting the two-layer system. From the ninth day, the three time-constants started forming. The first one started from 10⁵ to 10³ Hz, the second one began from 10³ to 1 Hz, and the third one started from 1 to 0.01 Hz, these time-constants contribute to the two layers of OA and BZI with the creation of aluminum oxide film on the interfacial metal surface.

3.5. Scanning Electron Microscopy (SEM)

Figure 6a–d show bare aluminum 2024 and sol-gel coated samples' after 360 h of immersion, SHX-80, OA-SHX-80, and BZI-OA-SHX-80, respectively. As shown in (a), the bare sample AA2024-T3 was attacked by corrosion in the form of aggressive deep pitting after 360 h immersion. Then in (b), the SHX-80 was sensitive to developing micro-cracks when dried in open atmospheric environments after immersion of 360 hr. These cracks were detected around 1–6 μ m wide on the surface, with some pitting appearing under it. Cracks can weakly affect the provided barrier corrosion protection of SHX-80, which has consequences for coatings' wet/dry cycling. Figure 6c shows that the OA-SHX-80 coating exhibited good resistance to corrosion and cracks under similar conditions. In addition, OA-SHX-80 was more robust than SHX-80. However, the coating after 360 h. started to fail. On the other hand, the Figure 6d, the BZI/OA sol-gel duplex system was durable and long-lasting for up to 60 days without appearing to be a visual crack or failure.

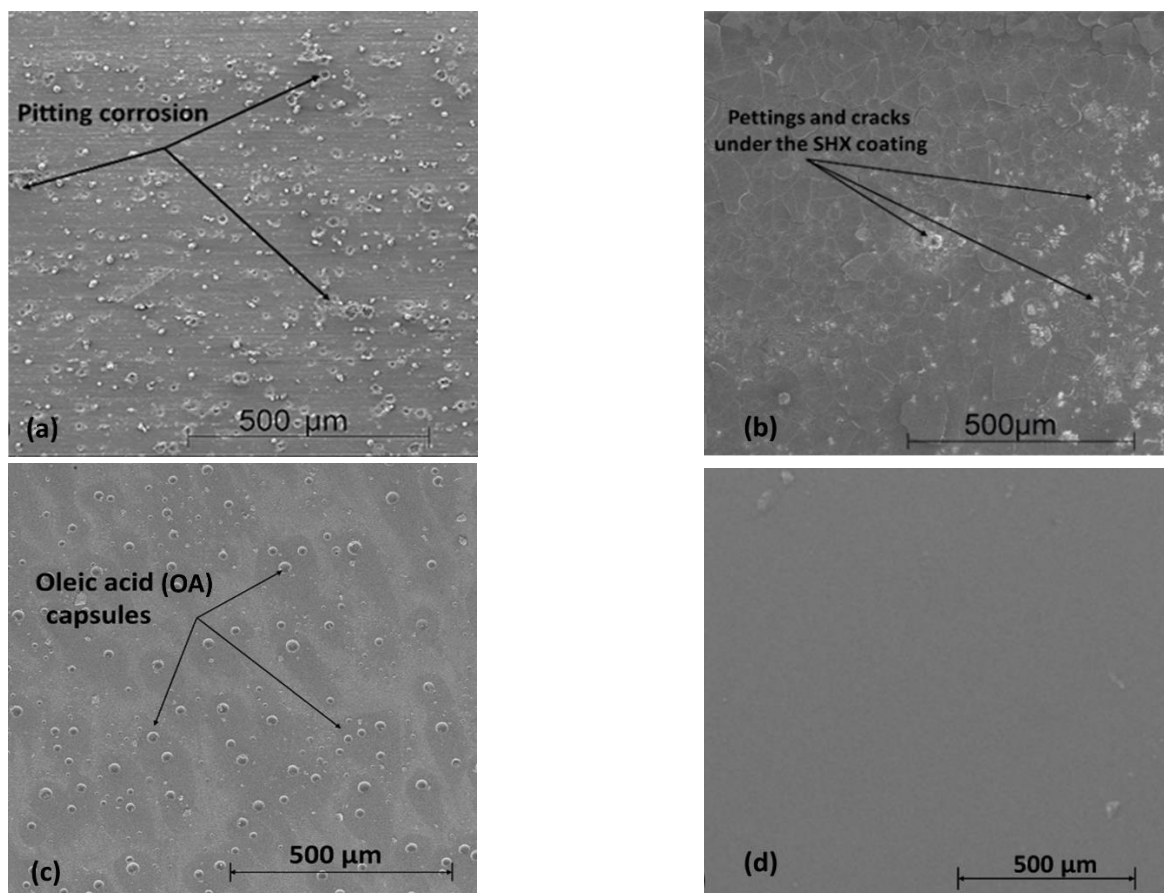


Figure 6. Surface morphology images for (a) bare AA 2024-t3, (b) SHX-80 coating, (c) OA-SHX-80, and (d) BZI-OA-SHX-80 coatings after 360 h. of immersion.

4. Conclusions

The silicate-based hybrid SHX Sol-gel can present typical barrier protection without any inhibitor. However, this protection can hold out for a maximum of ten days in 3.5% NaCl electrolyte solution before pitting, and cracking can be visually seen on the surface. Using OA only encapsulated the silica-based sol-gel revealed improved corrosion protection when combined with the base sol-gel coatings. Which mains the small amount of Octadec-9-enoic acid could enhance the sol-gel coating and provide protection over two weeks in an environment of 3.5% NaCl without any failure sign. Furthermore, Adding Octadec-9-enoic acid as an inhibitor to the sol-gel coating system can provide mimicked active protection due to the hydrophobicity and active molecule antioxidant of OA properties. However, the OA sol-gel coating after 360 h. of immersion fails to provide protection. Compared to all, the new developed duplex-silica-based hybrid coating system of benzimidazole/Octadec-9-enoic acid exhibited excellent anti-corrosion properties, providing an adherent protective film on the aluminium alloy 2024-T3 samples compared to the previous sol-gel in the same thickness and bare metals. This duplex system can last more than 60 days without any sign of failure with the same thickness as other sol-gel monolayer coatings, demonstrating that the duplex system is more durable than monolayer at the same thickness, with an eco-friendly and cost-effective.

Author Contributions: Methodology, M.H.M., O.L., and N.F.; revalidation and testing M.H.M., S.A.T., O.L., and N.F.; data analysis, M.H.M.; FTIR support, M.H.M., and S.A.T.; investigation, M.H.M.; resources, M.H.M.; writing, original draft preparation, M.H.M.; writing, review and editing, M.H.M., and S.A.T.; project supervision, N.F. and O.L. All authors have read and agreed to the published version of the manuscript.

Funding: This research has no direct funding.

Institutional Review Board Statement: Not applicable.

Informed Consent Statement: Not applicable.

Data Availability Statement: All data stored on the corresponding instruments and personal computers, and The data are not publicly available.

Acknowledgments: The authors would like to acknowledge the support of the Sheffield Hallam University in Material and Engineering Research Institute (MERI) and the Libyan Scholarship Program for financial support.

Conflicts of Interest: The authors declare no conflict of interest.

References

1. Polmear, I.; St. John, D.; Nie, J.-F.; Qian, M. Physical metallurgy of aluminium alloys. In *Light Alloys*; Butterworth-Heinemann, Elsevier Ltd.: Oxford, UK, 2017; pp. 31–107, ISBN 9780080994314.
2. Mussa, M. Development of Hybrid Sol-Gel Coatings on AA2024-T3 with Environmentally Benign Corrosion Inhibitors. Ph.D. Thesis, Sheffield Hallam University, Sheffield, UK, 2020.
3. Mussa, M.H.; Rahaq, Y.; Takita, S.; Farmilo, N. Study the Enhancement on Corrosion Protection by Adding PFDTES to Hybrid Sol-Gel on AA2024-T3 Alloy in 3.5% NaCl Solutions. *Albahit J. Appl. Sci.* **2021**, *2*, 61–68.
4. Brinker, C.J.; Scherer, G.W. *Sol-Gel Science: The Physics and Chemistry of Sol-Gel Processing*; George, W., Scherer, C.J.B., Ed.; 1st ed.; Academic Press: New York, NY, USA, 1990; Vol. 3.
5. Livage, J.; Sanchez, C. Sol-gel chemistry. *J. Non-Cryst. Solids* **1992**, *145*, 11–19.
6. Suleiman, R.; Khaled, M.; Wang, H.; Smith, T.J.T.; Gittens, J.; Akid, R.; Ali, B.M.E.; Khalil, A.; Mohamad El Ali, B.; Khalil, A. Comparison of selected inhibitor doped sol-gel coating systems for protection of mild steel. *Corros. Eng. Sci. Technol.* **2014**, *49*, 189–196.
7. Balaji, J.; Raja, P.B.; Sethuraman, M.G.; Oh, T.H. Recent studies on sol-gel based corrosion protection of Cu—A review. *J. Sol-Gel Sci. Technol.* **2022**, *103*, 12–38. <https://doi.org/10.1007/s10971-022-05818-9>.
8. Figueira, R.B.; Silva, C.J.R.; Pereira, E.V. Organic-inorganic hybrid sol-gel coatings for metal corrosion protection: A review of recent progress. *J. Coat. Technol. Res.* **2015**, *12*, 1–35. <https://doi.org/10.1007/s11998-014-9595-6>.
9. Hamdy, A.S.; Butt, D.P. Environmentally compliant silica conversion coatings prepared by sol-gel method for aluminum alloys. *Surf. Coatings Technol.* **2006**, *201*, 401–407.
10. Tiwari, A.; Hihara, L.H.; Atul, R.; Lloyd, H.; Tiwari, A.; Hihara, L.H. Sol-Gel route for the development of smart green conversion coatings for corrosion protection of metal alloys. In *Intelligent Coatings for Corrosion Control*; Tiwari, A., Rawlins, J., Hihara, L.H., Eds.; Intelligent Coatings for Corrosion Control; Butterworth-Heinemann: Boston, MA, USA, 2015; pp. 363–407, ISBN 9780124114678.
11. Talha, M.; Ma, Y.; Xu, M.; Wang, Q.; Lin, Y.; Kong, X. Recent Advancements in Corrosion Protection of Magnesium Alloys by Silane-Based Sol-Gel Coatings. *Ind. Eng. Chem. Res.* **2020**, *59*, 19840–19857. <https://doi.org/10.1021/acs.iecr.0c03368>.
12. EA Frame Evaluations of preservative engine oil containing vapor-phase corrosion inhibitor and a simplified engine preservation technique. In *Interim Report BFLRF No. 269*; EA Frame: San Antonio, TX, USA, 1991; pp. 19–131.
13. Mussa, M.; Zahoor, F.D.; Lewis, O.; Farmilo, N. Developing a Benzimidazole-Silica-Based Hybrid Sol-Gel Coating with Significant Corrosion Protection on Aluminum Alloys 2024-T3. *Eng. Proc.* **2021**, *11*, 9. <https://doi.org/10.3390/ASEC2021-11124>.
14. ASTM International. ASTM code B209—14 Standard Specification for Aluminum and Aluminum-Alloy Sheet and Plate. *ASTM Int.* **2016**, *25*, 16.
15. Mussa, M.H.; Farmilo, N.; Lewis, O. The Influence of Sample Preparation Techniques on Aluminium Alloy AA2024-T3 Substrates for Sol-Gel Coating. *Eng. Proc.* **2021**, *11*, 5. <https://doi.org/10.3390/ASEC2021-11121>.
16. Kumar, D.; Wu, X.; Fu, Q.; Ho, J.W.C.; Kanhere, P.D.; Li, L.; Chen, Z. Development of durable self-cleaning coatings using organic-inorganic hybrid sol-gel method. *Appl. Surf. Sci.* **2015**, *344*, 205–212. <https://doi.org/10.1016/j.apsusc.2015.03.105>.
17. Gutiérrez, E.; Rodríguez, J.A.; Cruz-Borbolla, J.; Alvarado-Rodríguez, J.G.; Thangarasu, P. Development of a predictive model for corrosion inhibition of carbon steel by imidazole and benzimidazole derivatives. *Corros. Sci.* **2016**, *108*, 23–35.
18. Obot, I.B.; Madhankumar, A.; Umoren, S.A.; Gasem, Z.M. Surface protection of mild steel using benzimidazole derivatives: Experimental and theoretical approach. *J. Adhes. Sci. Technol.* **2015**, *29*, 2130–2152.
19. Malik, M.A.; Hashim, M.A.; Nabi, F.; Al-thabaiti, S.A. Anti-corrosion Ability of Surfactants: A Review. *Int. J. Electrochem. Sci.* **2011**, *6*, 1927–1948.
20. Migahed, M.A.; Al-Sabagh, A.M. Beneficial role of surfactants as corrosion inhibitors in petroleum industry: A review article. *Chem. Eng. Commun.* **2009**, *196*, 1054–1075.